



OPEN

Determining the effect of aging, recovery time, and post-stroke memantine treatment on delayed thalamic gliosis after cortical infarct

Gab Seok Kim, Jessica M. Stephenson, Abdullah Al Mamun, Ting Wu, Monica G. Goss, Jia-Wei Min, Jun Li, Fudong Liu & Sean P. Marrelli✉

Secondary injury following cortical stroke includes delayed gliosis and eventual neuronal loss in the thalamus. However, the effects of aging and the potential to ameliorate this gliosis with NMDA receptor (NMDAR) antagonism are not established. We used the permanent distal middle cerebral artery stroke model (pdMCAO) to examine secondary thalamic injury in young and aged mice. At 3 days post-stroke (PSD3), slight microgliosis (IBA-1) and astrogliosis (GFAP) was evident in thalamus, but no infarct. Gliosis increased dramatically through PSD14, at which point degenerating neurons were detected. Flow cytometry demonstrated a significant increase in CD11b⁺/CD45^{int} microglia (MG) in the ipsilateral thalamus at PSD14. CCR2-RFP reporter mouse further demonstrated that influx of peripheral monocytes contributed to the MG/Mφ population. Aged mice demonstrated reduced microgliosis and astrogliosis compared with young mice. Interestingly, astrogliosis demonstrated glial scar-like characteristics at two years post-stroke, but not by 6 weeks. Lastly, treatment with memantine (NMDAR antagonist) at 4 and 24 h after stroke significantly reduced gliosis at PSD14. These findings expand our understanding of gliosis in the thalamus following cortical stroke and demonstrate age-dependency of this secondary injury. Additionally, these findings indicate that delayed treatment with memantine (an FDA approved drug) provides significant reduction in thalamic gliosis.

Abbreviations

pdMCAO	Permanent distal middle cerebral artery occlusion
GFAP	Glial fibrillary acidic protein
IBA-1	Ionized calcium binding adaptor molecule 1
NMDA	<i>N</i> -methyl- <i>D</i> -aspartate
TTC	2,3,5-Triphenyltetrazolium chloride
MG	Microglia

It is a well-accepted concept that ischemic damage can spread from the initial damage site (primary injury site) to remote areas which are functionally linked with the primary injury region. These remote lesions can develop over time, which trigger a variety of cellular responses in specific brain regions^{1,2}. Various cellular and molecular responses and injuries that aggravate neuronal and non-neuronal cell death are present in certain regions after stroke. These responses and changes in metabolic demand, neuro-inflammation, and cell death are mediated by excitotoxicity, reactive oxygen species (ROS) generation, apoptosis, necrosis, inflammations, glial cell activation, lymphocyte infiltration and blood brain barrier disruption, finally leading to neuronal loss^{1,3,4}.

The thalamus has received relatively little attention in the fields of stroke and neurodegenerative diseases, despite the thalamus' critical role in relaying signaling between different brain regions (e.g. cortex, hippocampus) as well as the spinal cord⁵. In addition, the thalamus is a key component in Papez circuits that are responsible for

Department of Neurology, McGovern Medical School, The University of Texas Health Science Center at Houston, 6431 Fannin St, Houston, TX 77030, USA. ✉email: Sean.P.Marrelli@uth.tmc.edu

memory and cognition^{5,6}. The phenomenon of secondary thalamic injury has been observed in human stroke^{7,8} and has been consistently detected in rodent stroke models in which specific regions of the cortex are injured^{9,10}. Multiple pieces of evidence suggest that this thalamic injury contributes to worsened outcome and recovery^{11,12}. Anatomically, the somatosensory cortex is connected to the thalamus via cortico-thalamic and thalamo-cortical projections^{13–15}. The cortico-thalamic projections that terminate in the somatosensory cortex originate from the ventral posterior nucleus (VPM) and posteromedial complex (PoM) of the thalamus^{16,17}. This region is generally regarded as a control center for bidirectionally relaying signals between cerebral somatosensory cortex and peripheral nerves and is critical for several brain functions, such as consciousness, sleep, and respiration^{18–20}. Moreover, emerging lines of evidence clearly show that the thalamus is not a mere passive relay center, but also serves as a critical hub for integrating and relaying the multimodal signals from other brain areas²¹. Dysfunction in the thalamus, caused by primary damage in cortex, is closely associated with poor outcome, degree of the disability and even decline of brain functions, such as cognition and memory²². For these reasons, secondary thalamic injury would reasonably be expected to impair recovery following stroke.

Recently, our studies as well as others have shown that neuronal damage can be observed in thalamus, along with severe gliosis and increased inflammation in an experimental stroke model^{23–25}. It has been speculated that many factors including ROS, excitotoxicity, and inflammation that is amplified by glial cell activation in a damaged cortex may provoke and initiate secondary injury in the thalamus¹⁰. However, detailed mechanisms and molecular changes in the thalamic area whereby cortical infarction leads to delayed injury in non-adjacent distant regions of brain are currently not well understood. As stroke predominantly occurs in the aged population, we compared the thalamic gliosis response in young and aged mice. Lastly, given the potential role of excitotoxicity in secondary injury, we further sought to test the applicability of memantine, an N-methyl-D-aspartate (NMDA) receptor antagonist, as a means for attenuating secondary injury and gliosis in thalamus after cortical stroke. Memantine is an FDA approved drug that is used in the treatment of Alzheimer's disease symptoms.

To our knowledge, this study represents the first demonstration that (1) primary cortical injury induces microglial proliferation and monocyte infiltration in the thalamus, (2) the resulting astrogliosis in the thalamus is likely permanent, (3) gliosis in aged stroke brains is reduced compared with young stroke brains, and (4) thalamic gliosis can be attenuated with delayed memantine treatment. These studies thus provide further molecular evidence supporting secondary injury as an important component of stroke pathology and provide new mechanistic understanding from which to design future therapeutic strategies.

Results

Cortical infarction promotes time-dependent changes in microglial activation in the thalamus. We evaluated the time course of microglial activation in the thalamus after cortical infarct. Region-specific microglial activation was visualized by immunostaining with an antibody against ionized calcium binding adaptor molecule 1 (IBA-1). IBA-1 is a microglia/macrophage-specific calcium-binding protein produced from the *Aif1* gene in microglia. In the brain, activated microglia express high levels of IBA-1 protein, whereas microglia in a resting state express a lower basal level. Figure 1A shows a coronal section from a post-stroke day 14 (PSD 14) brain immunolabeled for IBA-1. This coronal plane (-2 mm from bregma) contains the VPM and PoM nuclei of the thalamus and the posterior extreme of the cortical infarct²³. Note that microglial activation is prominent and well defined within the ipsilateral thalamus (Fig. 1A); similar activation was not found in the contralateral thalamus (data not shown). In the ipsilateral thalamus, IBA-1 + microglia exhibited typical morphological changes reflective of activated microglia (amoeboid shape and hypertrophied cell body), whereas the few IBA-1 + microglia in the contralateral thalamus exhibited resting morphology (Fig. 1B). We quantified the enlarged and hypertrophic MG in the thalamus after stroke by measuring microglial soma size. The microglial soma size of MG located in the ipsilateral thalamus, was significantly larger than those in the contralateral thalamus (Fig. 1C) ($P < 0.05$). Supplemental Fig. 1 shows 3D confocal images demonstrating these morphological characteristics in ipsilateral and contralateral thalamus at PSD 14. Examination of IBA-1 expression in brains from sham mice and PSD 3, 7, and 14 mice revealed that activated microglia were first evident in the ipsilateral thalamus at PSD 3 and became progressively more evident at PSD 7 and PSD 14 (Fig. 1D). We also used MG reporter mice (Cx3cr1-CreERT/tdTom) to evaluate MG expansion and morphology in the thalamus. Supplemental Figs. 2 and 3 show significant hypertrophy of the MG population in the ipsilateral thalamus at PSD 7. Together, these data show the delayed development of microglial activation within the ipsilateral thalamus, peaking beyond the time of primary cortical infarct and before the delayed neuronal injury in the thalamus (Supplemental Fig. 4).

Quantitative flow cytometry analysis demonstrates microglia in thalamus increase in number after stroke. Microglia are highly responsive to conditions found in the post-stroke brain (ischemic stress, pro-inflammatory cytokines, etc.). In the acute stroke phase (within 3 days after stroke) microglial cell number is significant reduced in the core and peri-infarct region due to massive microglial death by intensive ischemic damage and harsh hypoxic conditions^{26,27}. In the sub-acute to chronic stroke phase (e.g. beyond PSD 3), emerging lines of evidence suggest that microglia can proliferate in damaged regions of the cortex and migrate to ischemic core, where they produce a variety of cytokines and engage in cell debris clean up^{28,29}. However, it remains to be elucidated whether the increased IBA-1 + cells in the thalamus that we and others^{30–32} have shown reflects an increase in the proportion of activated microglia versus an increase in the total number of microglia. We therefore utilized flow cytometry to measure the number microglial cells from the thalamus and cortex of sham and PSD 14 brains. Cells were labeled with CD45 antibody and CD11b antibody to measure population changes in microglia as an indicator for microglial proliferation. The percentage of the microglia (CD45^{int}/CD11b⁺) among the total cell population in the thalamus was increased in stroke versus sham controls

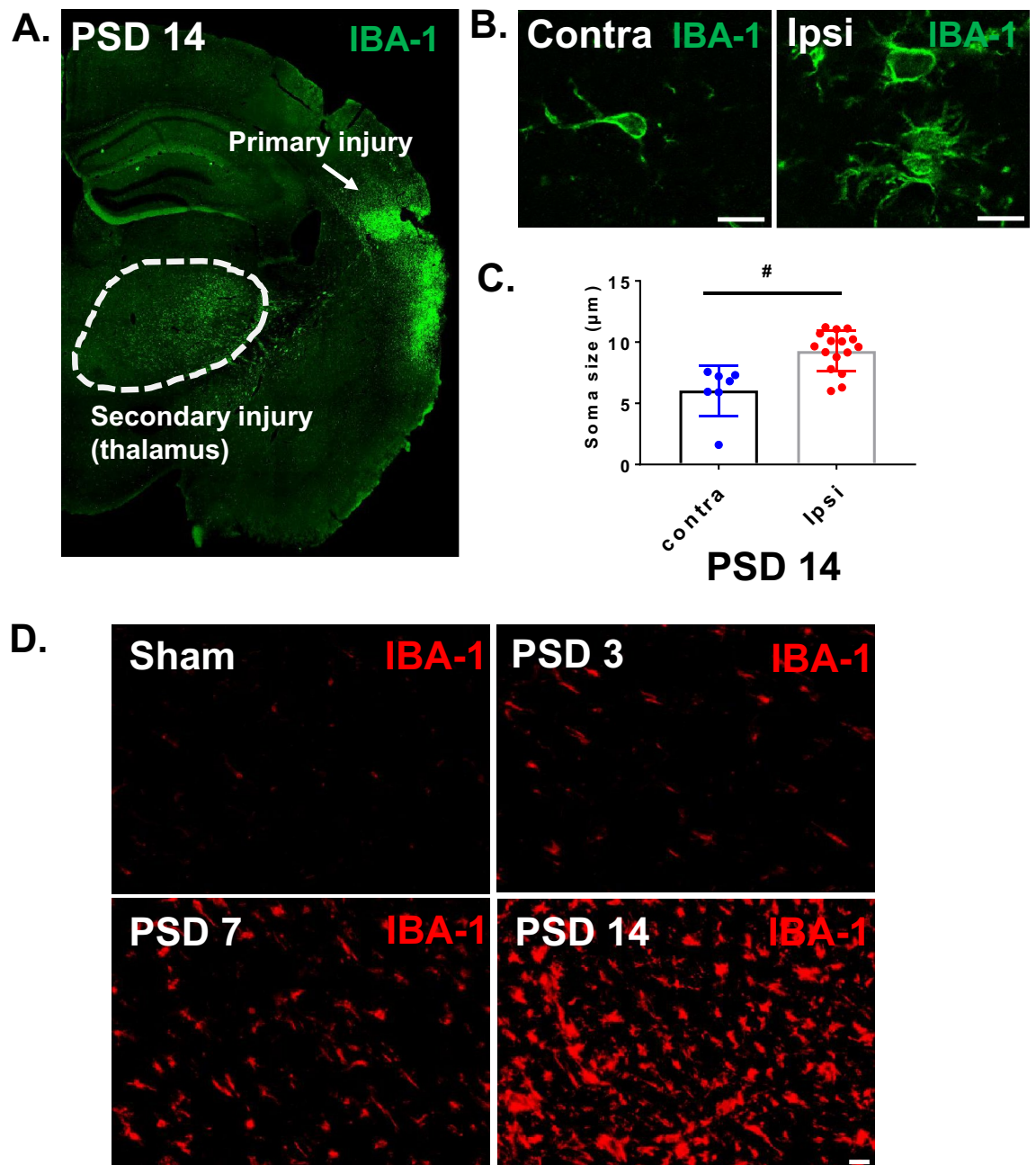


Figure 1. Cortical stroke induces delayed microglial activation in the thalamus. Cortical infarction was induced in young C57BL/6 J mice. At 3 days, 1 week and 2 weeks after stroke, brains were isolated and sectioned. Immunostaining with anti-IBA-1 antibody was performed. Brain sections at -2 mm from bregma were used for the visualization of thalamic microglial activation. **(A)** Coronal brain section showing activated MG/macrophages (IBA-1) in the posterior region of the primary injury and in the ipsilateral thalamus at PSD 14 (10X obj, stitched image). **(B)** Enlarged images showing morphology of MG/macrophages in the ipsilateral and contralateral thalamus at PSD 14 (scale bar = $10 \mu\text{m}$, 63X obj). **(C)** The microglial soma size, located in the ipsilateral thalamus, is much bigger than microglia in the contralateral thalamus ($\# p < 0.05$, unpaired t test) **(D)** Time course of IBA-1 staining showing delayed MG/macrophage activation in the ipsilateral thalamus (scale bar = $20 \mu\text{m}$).

(15.1% vs. 6.85%, $n = 6$) (Fig. 2A). We also found that the number of microglia counts in ipsilateral thalamus was increased compared to sham ($p < 0.05$, $n = 6$). In the ipsilateral cortex, there was a notable increase in the proportion of peripheral myeloid and lymphocyte cells, though the proportion or number of microglial cells ($\text{CD45}^{\text{int}}/\text{CD11b}^+$) was not significantly different from shams (Fig. 2B,C). These data support the possible role of either microglial migration into the region or microglial proliferation within the ipsilateral thalamus in the secondary injury after stroke.

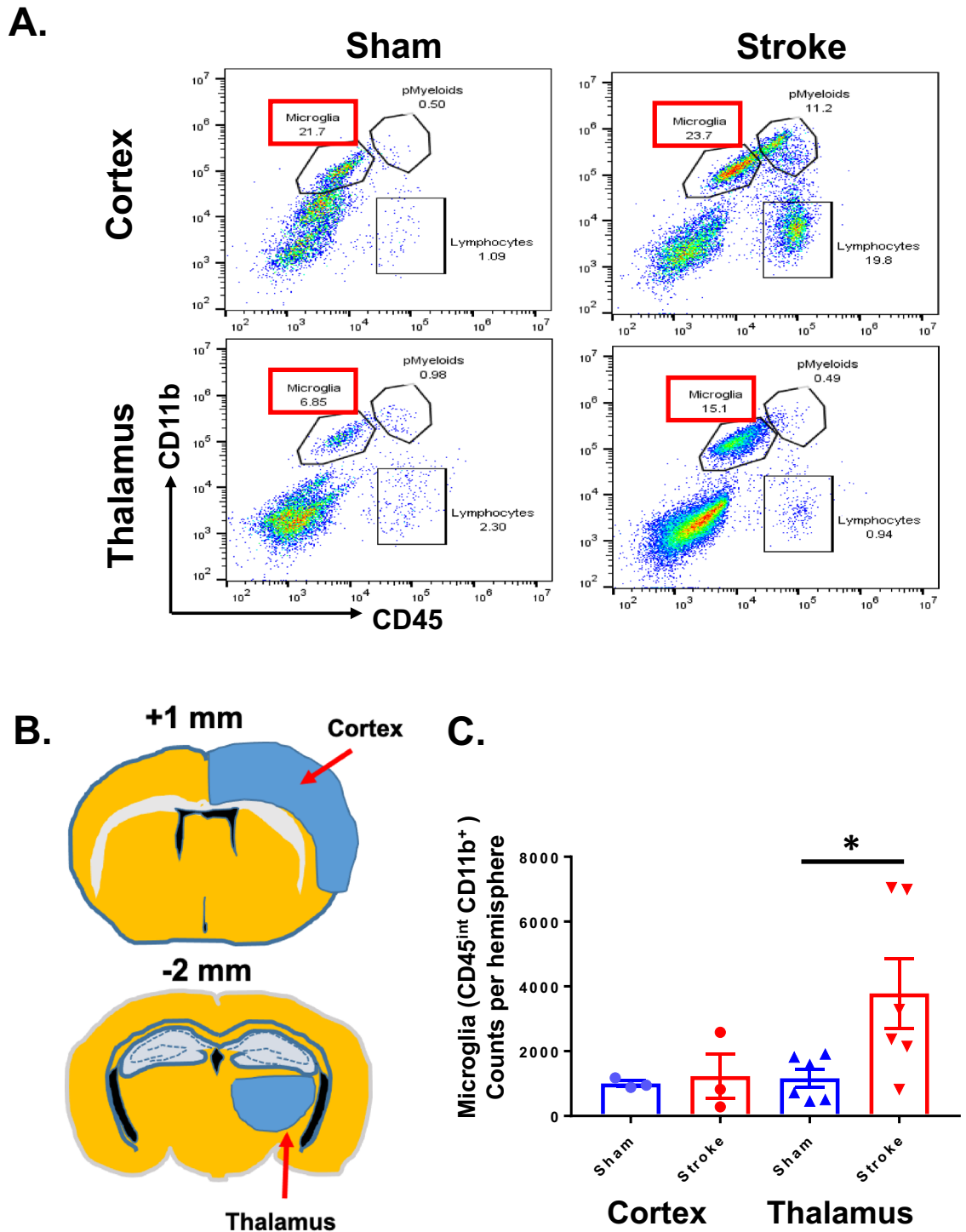


Figure 2. The resident microglial population increases in proportion and total number in the ipsilateral thalamus at PSD 14. At PSD 14, brains were harvested for cell cytometry. Single cell suspensions were obtained from cortex and thalamus. Cells were stained with CD45 antibody and CD11b antibody to measure the number and percentage of microglia in thalamus. (A) Representative cell cytometry plots generated from ipsilateral cortex and thalamus from sham and PSD 14 brains. The percentage of microglia, peripheral myeloid cells (pMyeloids), and lymphocytes is indicated numerically on the plots. (B) Illustration showing location of cortex and thalamus harvest sites from brain sections corresponding to +1 or -2 mm from bregma. (C) Number of CD45^{int}/CD11b⁺ cells in cortex and thalamus for sham and PSD 14 brains. * $P < 0.05$, unpaired t test.

Cortical stroke promotes recruitment of monocytes into the peri-infarct cortex as well as ipsilateral thalamus. It is known that peripheral monocytes can infiltrate the primary cortical injury and transform into IBA-1 expressing macrophages (M ϕ) after stroke^{33,34}. However, it is not clear if the increase in IBA-1 expressing cells in the injured thalamus reflects a similar invasion of peripheral monocytes. To determine if peripheral monocytes influx contributes to the secondary injury mechanism, we used reporter mice for peripheral monocytes. These mice express red fluorescent protein (RFP) under the control of the C–C motif chemokine receptor 2 (CCR2) promoter (CCR2^{RFP} mice)³⁵. We performed pdMCAO in CCR2^{RFP} mice and quantified the invasion of peripheral monocytes in the cortex and thalamus at PSD 14. As expected, we found the infiltration of RFP+ monocytes within the peri-infarct cortex (Fig. 3A). Interestingly, RFP+ monocytes were also significantly increased in the ipsilateral thalamus, compared to the contralateral thalamus in 2-week post stroke brains (Fig. 3B) or thalamus of naïve mouse brain (Fig. 3C). The number of infiltrated RFP+ cells were significantly increased in ipsilateral thalamus compared to contralateral thalamus: 147 (97 to 284) vs. 606 (466 to 951) (95% CI) cells per mm², n = 3, $p < 0.05$) after stroke (Fig. 3D). These data demonstrate that invasion of peripheral monocytes also contributes to the pathology of secondary thalamic injury.

Astrogliosis is evident in the thalamus after stroke. Astrogliosis is a well-documented phenomenon in primary ischemic stroke and has also been shown in secondary thalamic injury^{23,36}. Here we evaluated the time course of astrogliosis in secondary thalamic injury. Brains were harvested at PSD 3, 7, and 14 for immunostaining to glial fibrillary acidic protein (GFAP). GFAP is an intermediate filament protein which is upregulated in activated astrocytes and used to indicate astrogliosis. At PSD 14, the VPM and PoM nuclei of the ipsilateral thalamus demonstrated pervasive astrogliosis (Fig. 4A). In contralateral thalamus, similar astrogliosis was not found. The cortex, containing the posterior region of the primary infarct, also demonstrated significant astrogliosis and a dense glial scar. Earlier time points demonstrated astrogliosis in the ipsilateral thalamus by PSD 7, which continued to develop through PSD 14 (Fig. 4B).

Aged brains show reduced microglial activation in secondary thalamic injury. Multiple studies have shown that glial cell immune responses differ by brain region and with aging^{37,38}. Microglia in aged brains have been shown to be more proliferative and more easily activated to pro-inflammatory cytokine and immune conditions, especially in the damaged cortex^{39,40}. However, the effect of aging on microglial activation in secondary thalamic injury following stroke is not known. We compared pdMCAO brains at PSD14 from young and aged male mice. As expected, the young brains showed robust and pervasive microglial activation (IBA-1) across the ipsilateral thalamus (Fig. 5A). In contrast, although the aged brains showed strong IBA-1 expression in the primary cortical infarct region, the ipsilateral thalamus, showed less intense and less complete microglial activation. Comparison of IBA-1+ area showed a significant reduction in the ipsilateral thalamus of aged mice (Fig. 5B, n = 4–5, $p < 0.05$). These findings indicate that aged brains demonstrate dampened microglial activation in the thalamus, suggesting that microglial activation as a result of secondary injury may be attenuated in aging.

Aging reduces astrocytic activation in the thalamus following stroke. In order to explore how aging influences astrogliosis in the thalamus following stroke, we quantified activated astrocytes in the thalamus by GFAP immunostaining. We compared the degree of astrogliosis in the thalamus of aged and young brains following ischemic cortical stroke at PSD 7 and PSD 14. At PSD 7, astrogliosis in the thalamus of aged mice brains was significantly attenuated compared to that of young brains (Fig. 6A,B; n = 4–5, $p < 0.05$). Astrogliosis at PSD 14 trended to a reduction in the aged brains, but did not reach statistical significance. These data indicate that aging significantly attenuates the severity of astrogliosis in secondary thalamic injury following stroke.

Glial scar-like astrogliosis is observed in the thalamus of 2-year post-stroke brain. We have shown here and previously²³ that, unlike cortical astrogliosis (which includes diffuse gliosis and glial scar formation), the astrogliosis that occurs in the ipsilateral thalamus retains a more uniform pattern and lacks obvious scar characteristics. However, given the progressive development of astrogliosis that was observed over time, it was important to define the long-term characteristics of gliosis in this specific type of injury. Up to this point, glial scar formation is typically reported for primary injury to the cortex (ischemic and traumatic injury) or spinal cord injury. Therefore, to determine the long-term characteristics of astrogliosis in secondary thalamic injury, we compared GFAP immunoreactivity in mice at 6 weeks and 2 years post-stroke (young mice at the time of stroke). Astrogliosis in the ipsilateral thalamus at 6 weeks post-stroke was similar to that at PSD 14 (Fig. 7A). In particular, gliosis was widespread throughout the thalamic region, but without apparent glial scar characteristics. Note that glial scar was still evident at the site of primary infarct in the cortex, particularly in more anterior sections. At 2 years post-stroke, astrogliosis was still prominent in the ipsilateral thalamus (Fig. 7B). Interestingly, the gliosis had incorporated glial scar-like properties, including a dense scar core with surrounding reactive astrocytes (Fig. 7C). To our knowledge, this represents the first report of a glial scar in secondary thalamic injury. Astrogliosis was broadly elevated in the aged brains, particularly in the fiber tracts (e.g. corpus callosum, fimbria, internal capsule), hippocampus, and caudoputamen. However, note that gliosis in the contralateral thalamus was negligible compared to the ipsilateral thalamus. These data show that the astrogliosis that occurs as a result of secondary thalamic injury continues to evolve for months or possibly years, with the potential to develop scar-like features. In addition, the astrogliosis in secondary thalamic injury is extremely long-lasting, and possibly permanent.

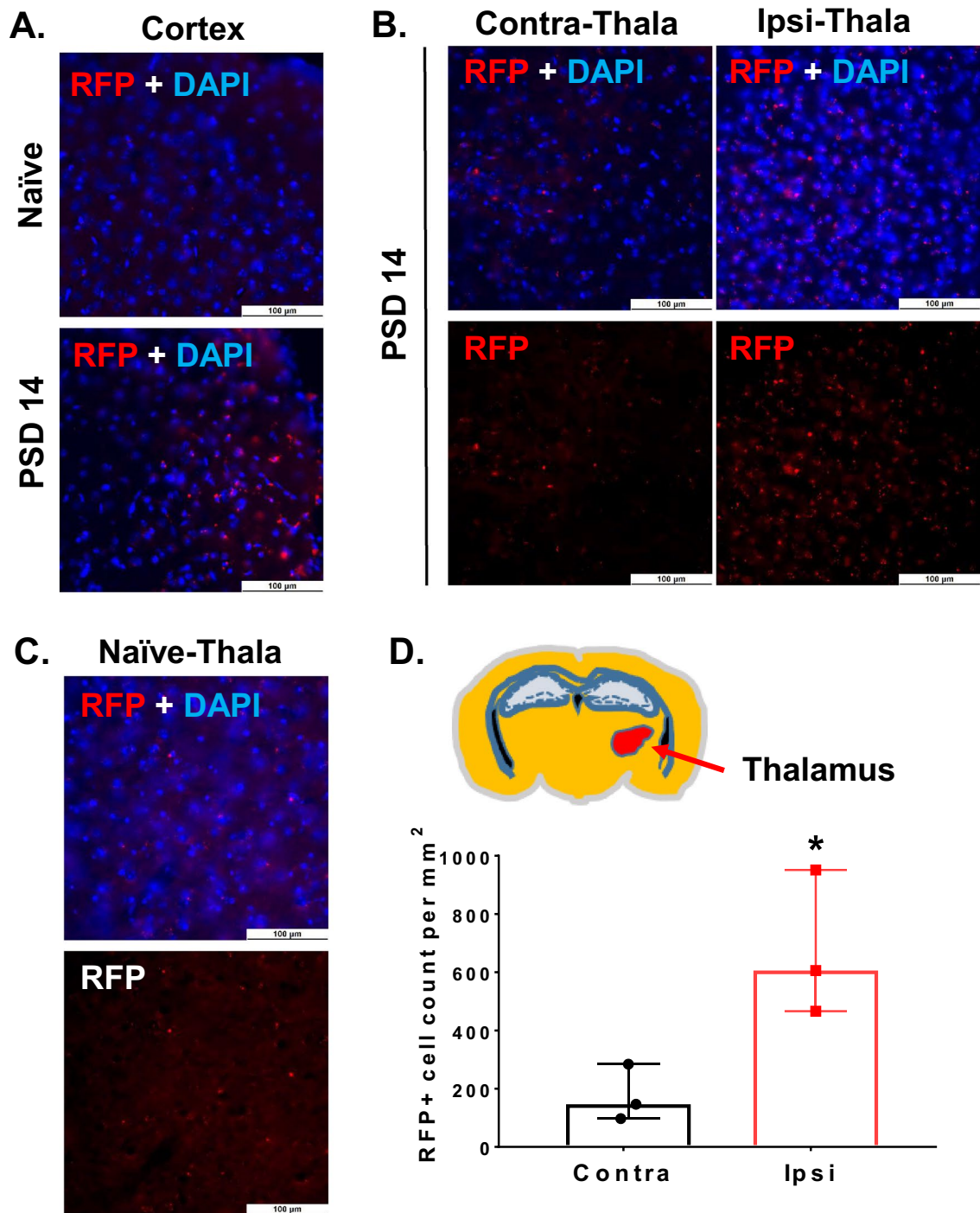


Figure 3. The ipsilateral thalamus demonstrates invasion of peripheral monocytes at PSD 14. CCR2-RFP reporter mice were used to track peripheral monocyte/macrophage invasion into the primary and secondary injury regions. CCR2-RFP mice underwent dMCAO and were evaluated at PSD 14. Representative images showing increased CCR2-RFP+ cells within (A) primary injury region (cortex) and (B) ipsilateral thalamus (20X obj; scale bar = 100 μ m). The frequency of CCR2-RFP+ cells in contralateral thalamus (B) was similar to that of naïve CCR2-RFP reporter mice (C). (D) Quantification of RFP+ cells demonstrating increased CCR2-RFP cells in ipsilateral thalamus (versus contralateral) at PSD 14. * $P < 0.05$, paired t test. Data expressed as median with 95% CI.

Thalamic gliosis can be attenuated with NMDA receptor antagonist following stroke. Secondary thalamic injury is thought to be mediated by the mechanisms of excitotoxicity, in part through NMDA pathways⁴¹. Therefore, we lastly sought to determine if the gliosis associated with secondary thalamic injury

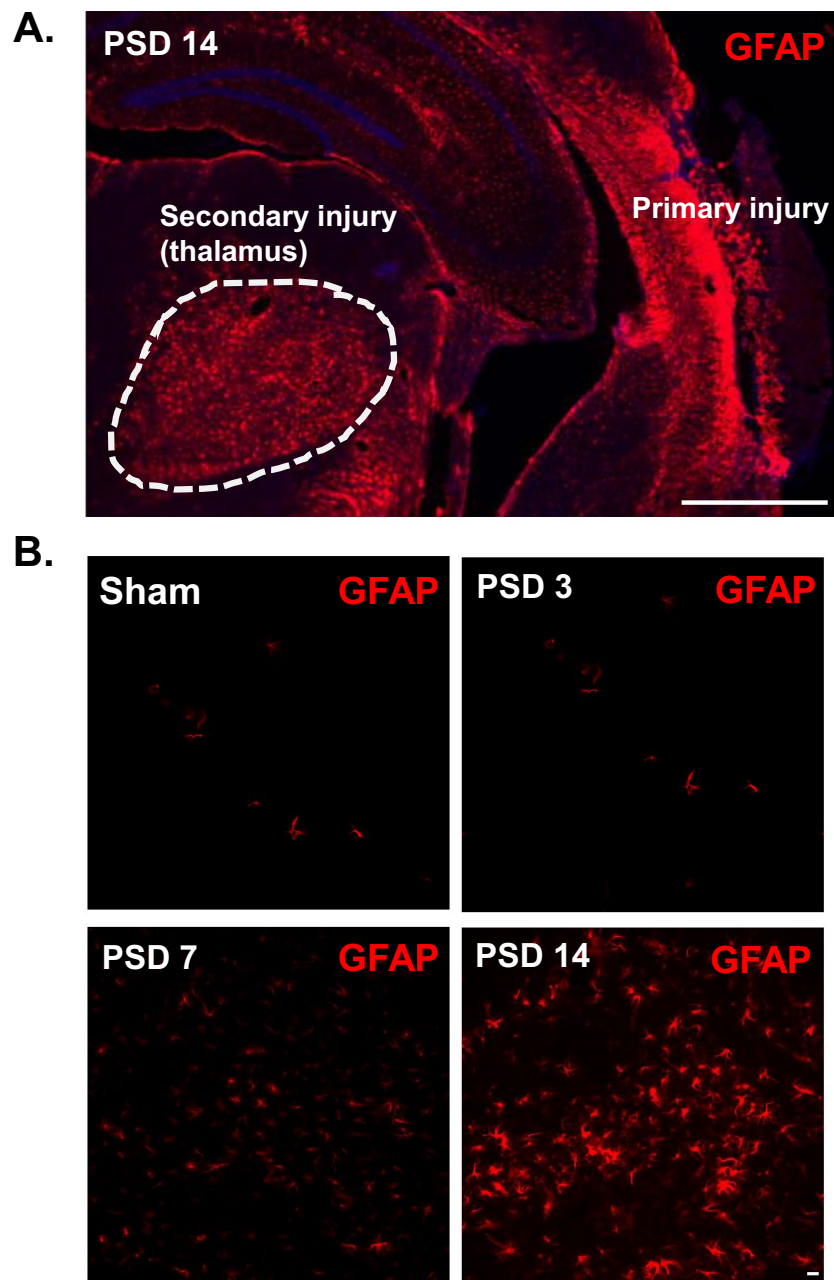
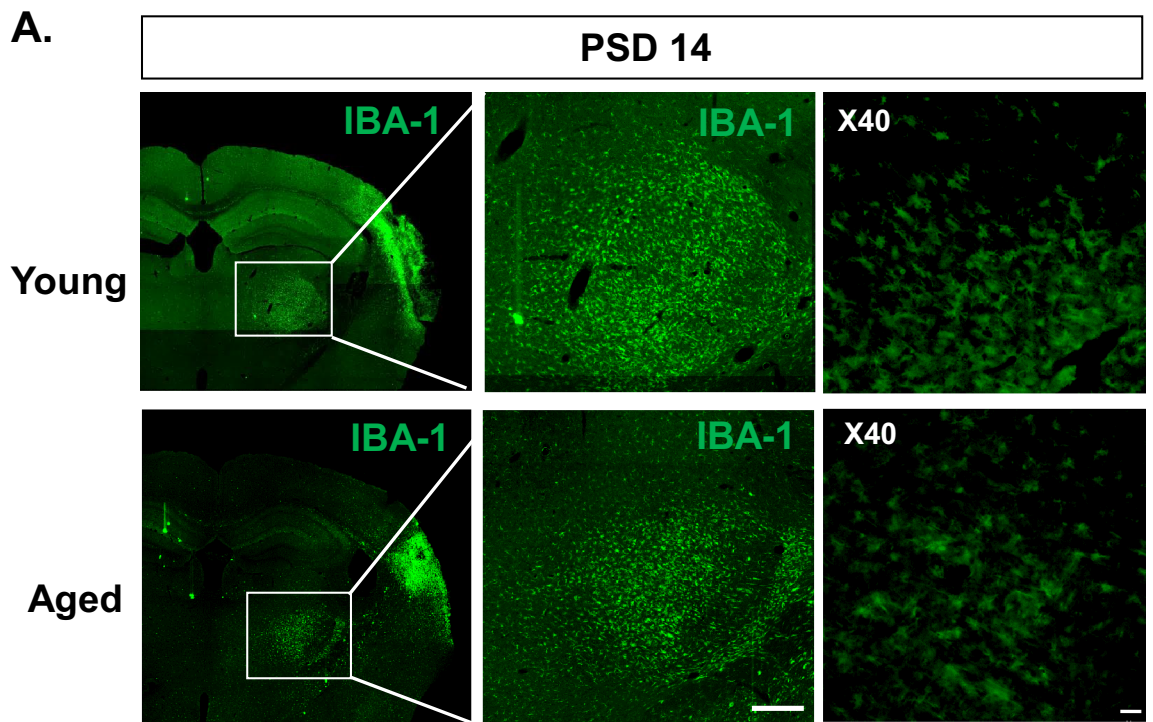


Figure 4. Cortical stroke induces delayed astrogliosis in the ipsilateral thalamus. Cortical infarction was induced in young C57BL/6 J mice. At 3 days, 1 week and 2 weeks after stroke, brains were isolated and sectioned. Immunostaining with anti-GFAP antibody was performed. Brain sections at -2 mm from bregma were used for the visualization of thalamic astrocyte activation. **(A)** Coronal brain section showing activated astrocytes (GFAP) in the posterior region of the primary injury and in the ipsilateral thalamus at PSD 14. A glial scar is evident in the cortical injury, but not within the thalamus (10X obj, stitched image; scale bar = 1 mm). **(B)** Time course of GFAP staining showing delayed astrocyte activation in the ipsilateral thalamus (20X obj; scale bar = 20 μ m).

could be reduced by treatment with a NMDA receptor antagonist (memantine). Memantine is an FDA-approved drug that has been reported to ameliorate primary cortical damage in preclinical stroke studies^{42–44} and has been proven safe in humans. In the clinical setting, memantine has been widely used for treating Alzheimer's disease (AD) patients, where it has been shown to reduce NMDA mediated neurotoxicity and inflammation and reduce symptoms of AD. Many studies have already shown that memantine reduces primary infarction and improves functional outcome in stroke animal models. To determine if memantine treatment can reduce secondary thalamic injury, we administered memantine (or vehicle) following pdMCAO in young mice. Memantine was delivered at 4 h post-stroke (100 mg/kg, ip) and again at 24 h post-stroke (50 mg/kg, ip). Brains were isolated at PSD 14 for quantification of cortical injury and thalamic gliosis. Infarct area was calculated in cresyl violet stained



B.

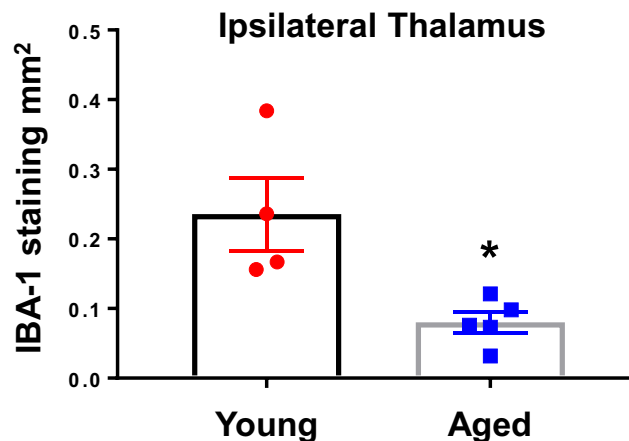


Figure 5. Aged mice demonstrate reduced IBA-1 expression in ipsilateral thalamus at PSD 14 compared with young mice. **(A)** Representative images comparing IBA-1 expression in brain of young (11–13 weeks) and aged (19–21 months) mice at PSD 14. Imaged with 10X obj, stitched image; scale bar = 1 mm (left panel) or 250 µm (middle panel). Blow up imaged with 40X obj; scale bar = 20 µm (right panel). **(B)** Quantification of total IBA-1 stained area in ipsilateral thalamus of young and aged mice. * $P < 0.05$, unpaired t test.

sections taken from the +1 mm from bregma position. Our previous study showed that this region of the cortex corresponded well with the severity of secondary injury in the thalamus (located in the -2 mm from bregma position)²³. Memantine treatment resulted in a slight reduction in infarct area of +1 mm sections, but did not reach statistical significance ($P = 0.065$) (Fig. 8A,B). Power analysis indicated that 18 samples would be required to achieve a power of 0.8 for this comparison. We also examined the effect of memantine on infarct volume in a separate cohort at PSD 3 (Supplemental Fig. 5). In this group, we found a similar non-significant trend for memantine reduction of total infarct or infarct in +1 mm sections ($P = 0.084$). The effect of memantine on reducing thalamic gliosis, however, was significant for both astrogliosis and microgliosis (Fig. 8C,D). Representative images are shown in Fig. 8 E,F and Supplemental Fig. 6. Together, these data demonstrate that secondary tha-

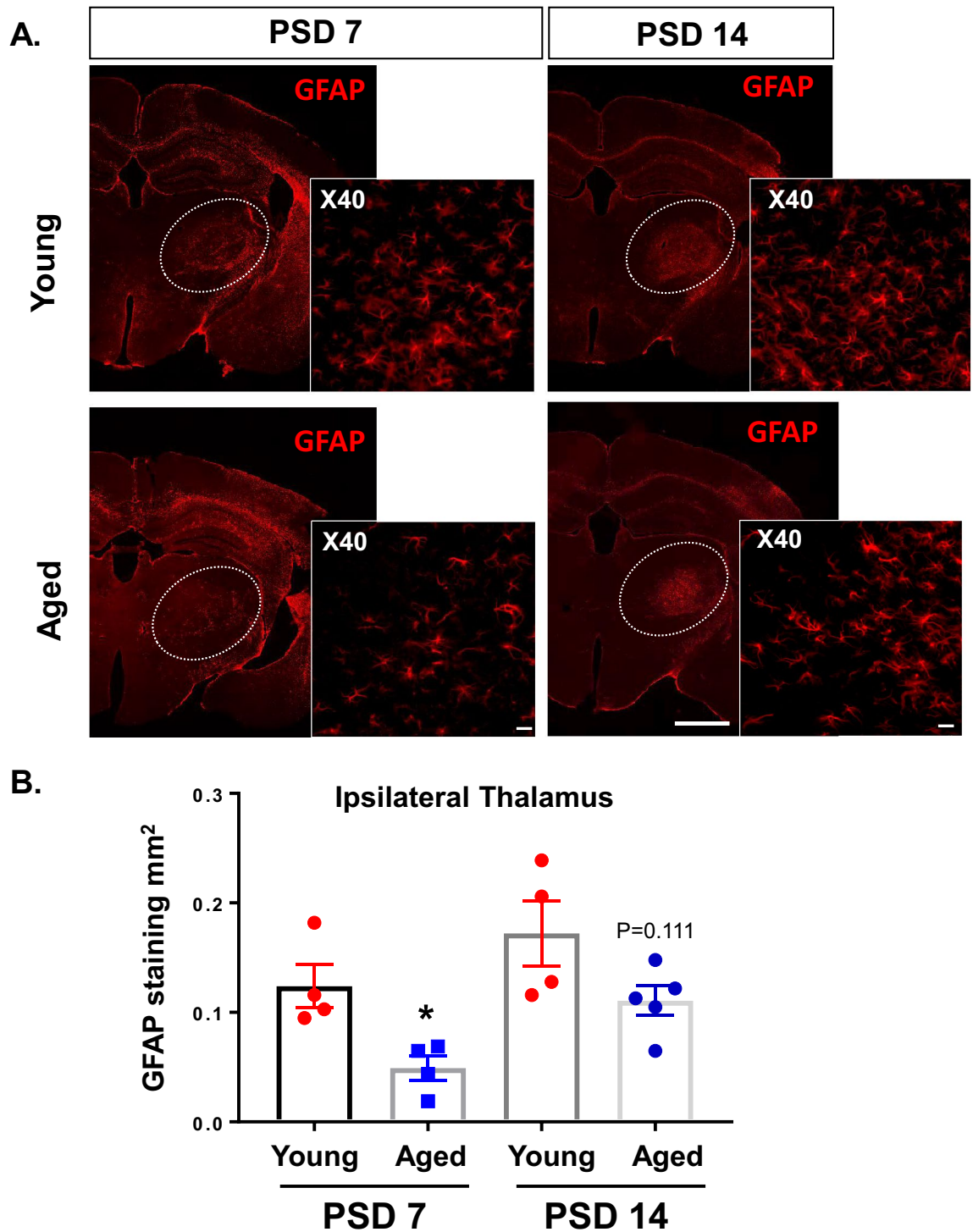


Figure 6. Aged mice demonstrate reduced astrogliosis in ipsilateral thalamus at PSD 7 compared with young mice. GFAP expression was evaluated at PSD 7 and PSD 14 in ipsilateral thalamus from young and aged mice. (A) Representative images showing GFAP expression in coronal sections at -2 mm from bregma (10X obj, stitched image; scale bar = 1 mm). Insert images were taken at 40X, scale bar = 20 μ m. (B) Quantification of total GFAP stained area in ipsilateral thalamus of young and aged mice. * $P < 0.05$, unpaired t test. ($P = 0.111$ for young versus aged at PSD 14).

lamic gliosis can be attenuated by pharmacologically targeting NMDA receptor activation (e.g. excitotoxicity) in the post-stroke period. These studies cannot definitively conclude whether the reduction of gliosis is due to a specific disruption of the secondary injury mechanism or if it is due to the possible reduction of primary injury.

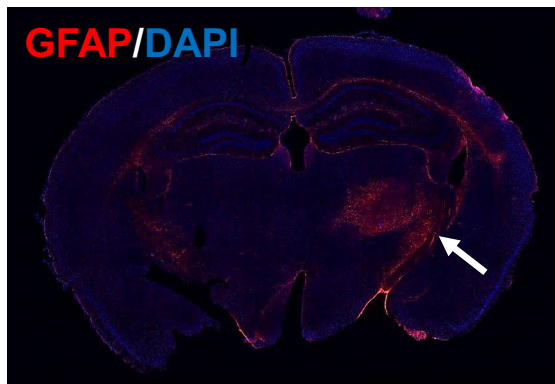
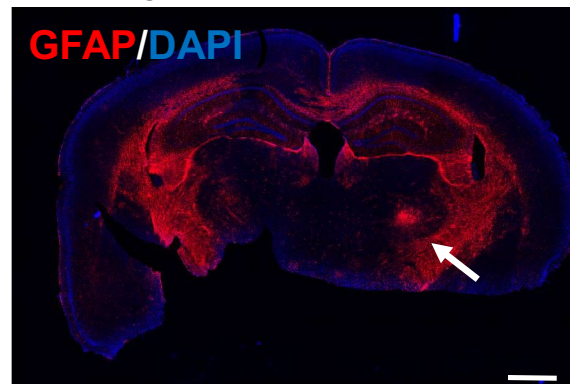
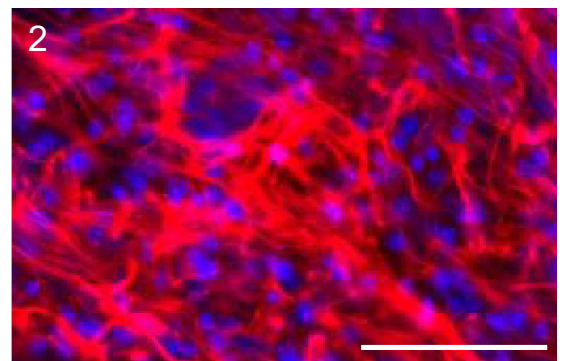
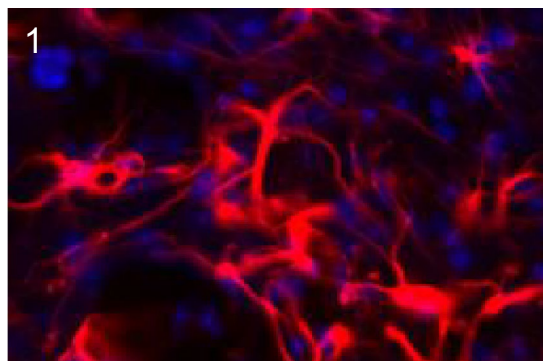
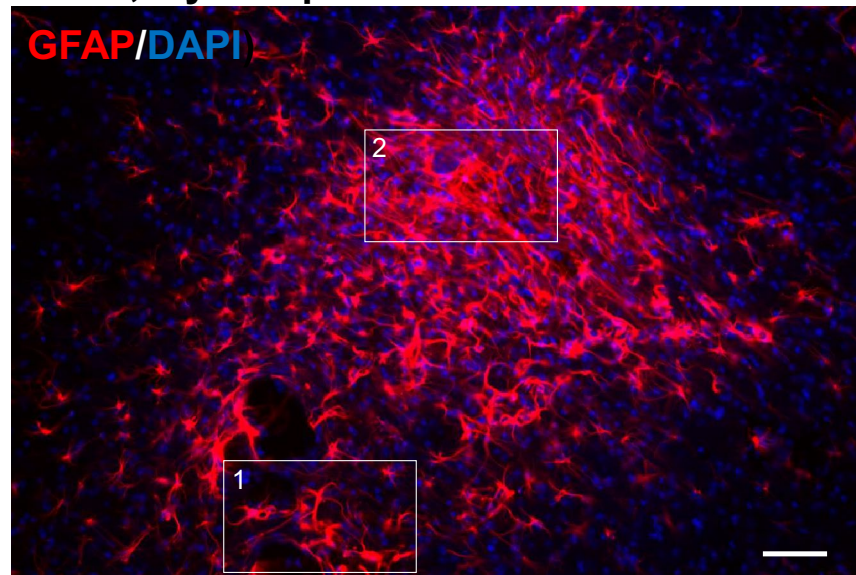
A. 6 weeks post-stroke**B. 2 years post-stroke****C. Thalamus, 2 years post-stroke**

Figure 7. Astroglial reactivity in ipsilateral thalamus is long-lasting and can eventually develop glial scar-like characteristics. Young mice were subjected to dMCAO and then allowed to recover for 6 weeks or two years. At 6 weeks or two years post-stroke, brains were evaluated for astroglial reactivity (GFAP). Brain sections showing astroglial reactivity at 6 weeks (**A**) or two years following stroke (**B**) (10X, stitched image; scale bar = 1 mm). (**C**) Enlarged region of thalamus from two year post-stroke brain showing glial scar-like characteristics (40X obj; scale bar = 50 μ m). Two regions (1 and 2) were further enlarged to show different regions of gliosis.

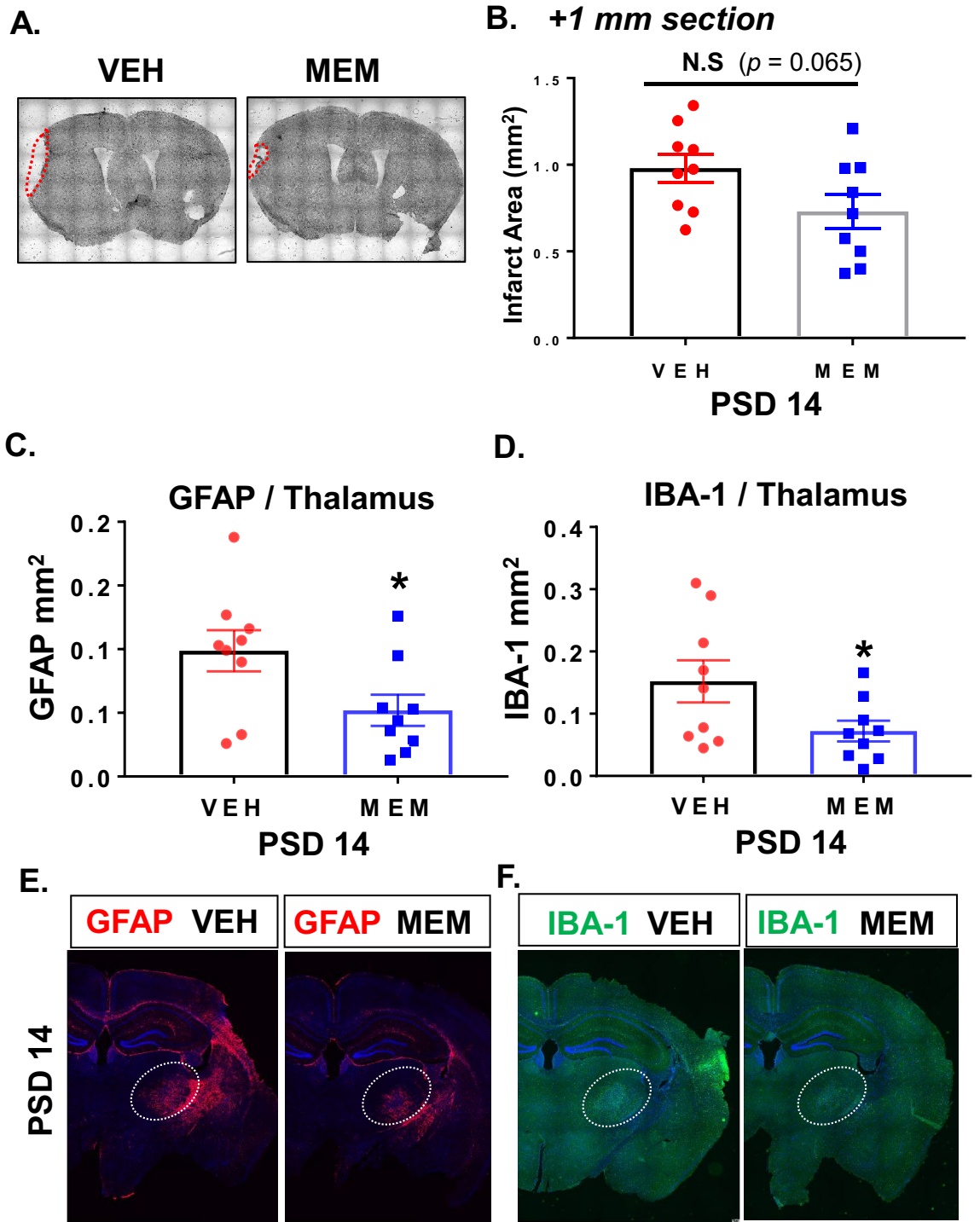


Figure 8. Memantine, an NMDA antagonist reduced glial activation in thalamus after stroke. Post-stroke treatment with memantine, an NMDA receptor antagonist, reduces gliosis in ipsilateral thalamus. Representative images showing CV staining (A) and infarct volume quantification at +1 mm section (B) at PSD 14 for memantine and vehicle treated mice. Primary cortical infarct volume was not significantly changed with memantine treatment ($n = 9, P = 0.065$, unpaired t test). Thalamic area demonstrating GFAP expression (C,E) and IBA-1 expression (D,F) was significantly reduced at PSD 14 with memantine treatment. * $P < 0.05$, unpaired t test.

Discussion

In this study, we explored the effects of aging and delayed memantine treatment on thalamic gliosis in a mouse stroke model of secondary injury. Using this model system, we made the following novel discoveries. First, we

showed that the gliosis response in the thalamus consists of a significant expansion of the microglia/macrophage cell population, which is due in part to the invasion of peripheral monocytes. Second, we showed that the thalamic gliosis response is attenuated in aged mice. Third, we demonstrated that astrogliosis in the ipsilateral thalamus is long-lasting (possibly permanent) and eventually develops glial scar-like characteristics. Fourth, post-stroke treatment with NMDA receptor blocker, memantine, attenuates gliosis in the thalamus. We expand on these new findings below.

The gliosis response in the thalamus consists of a significant expansion of the microglia/macrophage cell population, which is due in part to the invasion of peripheral monocytes. It is well-established that CNS injury initiates the intrinsic programs for microglia to act as a first response immune cell in the brain. In this process, activated microglia play a critical role in sensing neuro-inflammation and releasing chemokines and cytokines (pro- and anti-inflammatory), which spread from the damaged area to the spared but active brain area^{45,46}. A large body of evidence on how microglial phenotypes are altered by ischemic injury explains the regional diversity and modes of microglial polarization from M0 to M1 or M2 in neurodegenerative disease models, in response to the severity and types of injuries^{47,48}. During the acute stroke phase, the ischemic stress causes microglia in the core and penumbral regions to undergo apoptosis and necrosis, thus resulting in the decrease in microglial cell number^{26,27}. Subsequently, the microglial cell population can return through proliferation of remaining MG or migration of MG from nearby regions^{49–51}. In addition, CCR2⁺ peripheral monocytes can infiltrate the injury region and then differentiate into macrophages or microglia-like cells^{34,52,53}. The differentiation of the macrophages is affected by the local environment as well as the type and time course of injury⁵⁴. Whether peripheral monocytes invade or contribute to a microglia/macrophage population in *secondary* injury is not currently known.

We used a combination of immunostaining, flow cytometry, and CCR2 reporter mice to examine the temporal and cellular origin of gliosis in the thalamus after stroke. Similar to what others have shown, the cortical infarct induced delayed and progressive microgliosis (IBA-1⁺ cells) within the VPM/PoM nuclei of the ipsilateral thalamus^{30,55}. Using flow cytometry, we found that the proportion and absolute number of CD45^{int}/CD11b⁺ MG was significantly increased in PSD 14 thalamus. The CD45^{int}/CD11b⁺ cells are reflective of the total MG population, not simply the activated MG (i.e. IBA-1⁺ cells). The four-fold increase in total MG in the ipsilateral thalamus (versus sham) indicates a substantial expansion of this population above pre-injury levels. In comparison, the absolute number and proportion of CD45^{int}/CD11b⁺ MG in cortex at PSD 14 was similar to sham controls. The cause of this difference between cortex and thalamus was not determined, but could reflect a less extensive (or no) initial MG depletion following thalamic injury or a different time course of MG depletion/repopulation. In addition, the proportional value of MG in the cortex sample reflects a dilution effect from the increase in peripheral myeloid cells and lymphocytes. Therefore, to more specifically evaluate the region and injury-specific potential for peripheral monocyte invasion, we performed pdMCAO in CCR2 reporter mice. These mice express RFP in CCR2-expressing monocytes and monocyte lineage cells (e.g. monocyte-derived macrophages), but not in resident CCR2-negative macrophages. As expected, the cortex demonstrated the presence of RFP⁺ monocyte/macrophages at PSD 14. Interestingly, the ipsilateral thalamus also demonstrated a significant increase in RFP⁺ cells, indicating that peripheral monocytes do invade the thalamus following secondary injury. To our knowledge, this represents the first report of peripheral monocyte infiltration as part of the secondary injury mechanism. In primary stroke injury, circulating CCR2⁺ monocytes have been shown to be recruited to ischemic regions from the leptomeninges surrounding the brain parenchyma and then along penetrating arterioles³⁴. However, given the greater distance of the thalamus from the leptomeninges, monocyte influx from the blood circulation may be more likely in this brain region. Nevertheless, regardless of how the monocytes ultimately arrive, these findings suggest that peripheral monocytes can contribute to the expansion of the IBA-1⁺ MG/Macrophage population in secondary injury in the thalamus. Future studies are warranted to determine the signaling mechanisms and route of entry for recruited peripheral monocytes, the time course of monocyte infiltration, and the role of this monocyte-derived population in the mechanism of secondary injury or repair.

The thalamic gliosis response is attenuated in aged mice. The risk of ischemic stroke is greatly increased in aging, showing a doubling of stroke incidence for each decade after 55 years of age⁵⁶. Therefore, to increase the translational value of these studies, we performed a subset of studies in aged mice (18–22 months). This age range in mice corresponds roughly with that of humans in the 6th to 7th decade of life^{57,58}.

Aging is associated with a number of pathological changes in MG and astrocytes, two glial cell types which play important roles in both brain support and response to injury^{59,60}. Much of the age-dependent increase in neuroinflammation has been linked to changes in microglia, which exhibit both morphological and molecular changes consistent with an enhanced inflammatory profile⁶⁰. These “primed” phenotype MG in the aged brain demonstrate increased expression of antigen presentation and antigen receptor genes and demonstrate an exaggerated inflammatory response to immune stimuli⁶¹. Astrocytes also demonstrate age-dependent impaired support function and exaggerated responsiveness to injury. Aged astrocytes produce lower amounts of trophic factors, such as VEGF and Wnt3, exhibit reduced glutamate uptake and clearance, and contribute to accelerated glial scar formation⁵⁹. In general, aging leads to a brain environment in which glial support function is reduced and responsiveness to inflammatory stimuli is amplified. However, evidence for how aging affects the MG and astrocytes response in secondary injury is currently lacking.

We showed that aged mice, despite the formation of a classic glial scar in the cortex, exhibited reduced astrogliosis and microgliosis in the thalamus following stroke. Given the enhanced inflammatory responsiveness in the aged brain, this outcome was contrary to our initial prediction. However, a possible explanation for the reduced gliosis response may involve age-dependent cell senescence, as some reports have shown MG senescence and

hypoactivation in aging^{60,62,63}. In addition, MG in the aged CNS have also been reported to have reduced potential for replication due to telomere shortening and demonstrate reduced proliferation following injury^{63,64}. The combination of reduced activation and reduced proliferation, could account for the reduced IBA-1 + population in the ipsilateral thalamus and a reduced source of inflammatory stimulation of astrocytes. To our knowledge, our study represents the first report of how aging specifically affects the pathology of secondary thalamic injury.

Astrogliosis in the ipsilateral thalamus is long-lasting (possibly permanent) and eventually develops glial scar-like characteristics. The astrogliosis response in the thalamus consisted of a diffuse distribution of GFAP⁺ astrocytes throughout the VPM and PoM nuclei, becoming first evident between PSD 3 and 7. The astrogliosis in thalamus differed from that in the primary cortical injury region in that a glial scar did not form around the injury within the first two weeks, or even 6 weeks. However, at two years after injury, a dense highly-GFAP⁺ cell cluster developed within the ipsilateral thalamus. This cluster demonstrated the dense mesh-like arrangement of activated astrocytes characteristic of a glial scar⁶⁵. The contralateral thalamus was notably lacking in gliosis, thus supporting the causative role of the primary stroke injury on the enduring gliosis in the ipsilateral thalamus. While the aged brains did show increased astrogliosis in a variety of brain regions (particularly in the fiber tracts), it showed bilateral distribution.

The formation of a glial scar is a common feature in primary stroke injury, as well as several other types of severe injury in the CNS^{65–68}. The glial scar is composed mainly of hypertrophic astrocytes which characteristically express increased levels of GFAP⁶⁵. The scar typically forms at the boundary between necrotic and healthy tissues and appears to support tissue repair mechanisms in the CNS^{69,70}. However, how the scar either impedes or supports axon regrowth is still hotly contested⁶⁹. The cause or purpose of glial scar formation in the thalamus is perplexing. The scar in this region appears to take many months (or possibly years) to develop; thus, the purpose appears to be inconsistent with that of a protective barrier to support repair. Given that the scar was shown in mice two years following stroke, it is possible that the slow development of the scar might be related to the changing environment within the aging brain. Given the reported role of JAK-STAT3 in scar development in ischemia injured cortex and injured spinal cord, it would be interesting to determine if the delayed scar formation is also associated with a delayed induction of the STAT3 pathway^{71–74}. In light of the lengthy time over which this secondary injury develops, it will be important to evaluate the potential to either reduce (i.e. therapeutic) or worsen (i.e. environmental stress, etc.) secondary injury at significantly later time points.

As a result of the advent of new technologies, such as comprehensive single cell RNA sequencing and large-scale transcriptome analyses, we are gaining a better appreciation of the clear heterogeneity in astrocytes in CNS. This heterogeneity, which is driven by physiological and pathological conditions as well as aging, accounts for specialized functions of these cells in different brain regions, circuits and networks^{75,76}. Thus, each type of astrocyte can play a unique role in sensing and responding to the diverse cellular signaling, which occurs in different steps of inflammatory responses. The formation of the glial scar is an example of specialized astrocytic function in the context of stroke. It is well established that the glial scar, which forms around the infarcted area, contributes to the inhibition of the spread of inflammation to nearby healthy tissue, the production of neurotrophic factors in repair/remodeling, and the generation of a scaffold for facilitating axonal regrowth^{77,78}. However, as noted above, the injury within the ipsilateral thalamus showed broad astrocyte activation, but no evidence of glial scar formation—even through six weeks after stroke. The reason for the different gliosis pattern may reflect different types of injury (ischemic vs. excitotoxic) as well as different subtypes of glial cells in the respective regions. A recent study using scRNAseq revealed seven distinct types of astrocytes with region-specific distributions in the brain⁷⁵. The authors found that two major sub-types of astrocyte populations (telencephalon astrocytes) are distributed in the cortex, striatum, amygdala, and hippocampus. However, they showed that these sub-types are absent in the thalamus and midbrain, highlighting the heterogeneity of astrocytes in the cortex and thalamus.

Post-stroke treatment with NMDA receptor blocker, memantine, attenuates gliosis in the thalamus. The thalamus plays many critical roles in the brain, and serves as a vital relay station between different brain regions (e.g. cortex and brainstem). However, as a result of the high connectivity of this brain center, the thalamus is also vulnerable to secondary injury from multiple brain regions. Remote secondary thalamic injury has been observed in rodent stroke models as well as in human stroke pathology. Furthermore, thalamic dysfunction is associated with worsened outcome and recovery following stroke^{7,9,79}. It is significant to note that the development and progression of this secondary injury appears to be modifiable in experimental models. We have previously shown that thalamic injury (neuronal loss and gliosis) can be reduced with post-stroke hypothermia²³, while others have shown similar benefit with low oxygen post conditioning⁴¹. In the other direction, others have shown that the neuronal loss can be enhanced by 4 weeks of post-injury chronic stress²⁴.

From a clinical perspective, the slow development and modifiable nature of secondary injury is encouraging, as it means this type of injury is amenable to delayed therapeutic interventions.

Memantine is an NMDA receptor antagonist that has been previously demonstrated to reduce primary infarction in experimental models of both permanent and transient stroke models^{42–44}. This drug is also currently used clinically in the treatment of Alzheimer's disease symptoms⁸⁰. Although the mechanism of secondary injury is not fully elucidated, it does appear that glutamate-mediated excitotoxicity plays a key causative role⁸¹. Whether post-stroke treatment with memantine could reduce the secondary thalamic injury and gliosis has not previously been studied.

Our studies indicated that treatment with memantine at 4 and 24 h after stroke results in reduced gliosis in the ipsilateral thalamus. Both astrogliosis and microgliosis was significantly reduced in memantine treated mice. The primary cortical infarct at +1 mm from bregma (containing the cortical region with the majority of thalamocortical projections) appeared somewhat reduced, but failed to reach statistical significance. A separate

cohort examined at PSD 3 showed a similar trend with memantine treatment. The high variability of the memantine response may indicate that it is effective in reducing primary injury, but that the dosing or timing may be suboptimal. Given the potential that memantine reduced the primary injury in our studies, we cannot definitively conclude if the significant reduction in thalamic gliosis was a result of reduced primary cortical injury or a specific disruption of the progression of secondary injury. Future studies would be required to tease apart these two possibilities. However, regardless of the aforementioned distinction, it is encouraging that memantine delivered four hours after stroke was effective in reducing thalamic gliosis.

Limitations. Our studies were performed exclusively in male mice. However, it has been shown that there are sex differences in microglial and astrocyte responses to ischemic injury, in both inflammatory response and cell survival following ischemic stress^{82–84}. Future studies will be required to determine how secondary thalamic injury is affected by sex hormones or genetic sex.

Summary. Secondary injury can be produced in distal brain regions via interconnecting neuronal pathways with primary sites of ischemic injury. Relay centers, such as the thalamus, may therefore be particularly vulnerable to this type of injury. We found that cortical stroke induces progressive and lasting gliosis associated with secondary injury in the ipsilateral thalamus. This thalamic injury is characterized by initial gliosis, followed by neuronal loss in the VPN and PoM nuclei. Over a period of several months, the gliosis in the thalamus eventually develops characteristics of a glial-scar. In aged mice (aged at the time of stroke), gliosis in the thalamus is attenuated. We also showed for the first time that peripheral monocytes invade the injured thalamus and can therefore contribute to the expansion of the activated microglia/macrophage population in secondary injury. Lastly, we showed that post-stroke treatment with an NMDA receptor antagonist results in reduced gliosis in the thalamus. These findings provide an important foundation for future studies on the molecular mechanisms of thalamic injury and for strategies aimed at reducing secondary brain injury after stroke.

Methods

Animals. All procedures were performed in accordance with NIH guidelines for the care and use of laboratory animals and were approved by the Institutional Animal care and use committee of the University of Texas Health Science Center. In vivo study was carried out in compliance with the ARRIVE guidelines. Male C57BL/6 J mice (11–14 weeks old and 18–22 month old) were used for all experiments. All animals were housed in the animal care facility and had access to water and food ad libitum at University of Texas Health Science Center. For the PSD 14 memantine study, we randomly assigned animals to treatment groups (Vehicle; 10 mice, Memantine; 10 mice, 11–14 weeks old mice). One mouse in vehicle group and one mouse in the memantine group died during the stroke surgery and were excluded from the study. For the PSD 3 memantine study to measure primary infarction, we randomly assigned a total 12 mice to vehicle or memantine groups (Vehicle, 6 mice, Mem, 6 mice). One mouse in the vehicle treated group died during surgery and was excluded from the study. In addition, four male Cx3cr1-TdT mice were used in this study (a microglia TdTomato reporter line).

Permanent distal middle cerebral artery occlusion (pdMCAO) model. We used male C57BL/6 mice, between 11 and 14 weeks (young) or 18–22 months (aged). Permanent focal cerebral ischemia was induced by permanent occlusion of the right distal middle cerebral artery (MCA) using electro-coagulator. The distal MCA was accessed via a craniotomy and permanently occluded just proximal to the anterior and posterior branches. Mice were anesthetized with isoflurane (4% induction and 2% maintenance in airflow) during the surgery. Body temperature (rectal probe) was maintained at 37 °C during surgery. Bupivacaine (1 ml/kg of 0.25% solution, s.c.) was injected prior to skin incision for pain management. A skin incision was made between the ear and eye and the temporal muscle was detached from the skull to locate the MCA beneath the transparent skull. A small craniotomy was then generated over the MCA using a micro-drill to provide access to the artery. An Accu-temp variable low temperature cautery was used to permanently ligate the MCA. After surgery, mice received heat support for 2 h. Sham controls underwent the same procedure, except for the ligation of the MCA.

5-Triphenyltetrazolium chloride (TTC) staining. Brains were harvested and cut into 1 mm-thick slices using a mouse brain matrix (Harvard Apparatus, MA, USA). Brain slices were incubated in a 1% 2,3,5-triphenyltetrazolium chloride (TTC) solution in phosphate buffered saline for 30 min. TTC is converted by active mitochondria to a red compound, thereby staining metabolically active tissue red and leaving infarcted tissue white. Stained slices were imaged for calculation of infarct volume in Image J (National Institutes of Health, Bethesda, MD).

Fluoro Jade C staining. Fluoro-Jade C (FJC) was prepared from the powder form (AG325, MiliporeSigma, MO, USA) and used to detect degenerating neurons. Brain slices were incubated with 100% ethanol followed by 70% ethanol. Sections were then incubated in 0.06% potassium permanganate solution for 10 min. After washing with distilled water, sections were incubated in a 0.0001% solution of FJC dissolved in 0.1% acetic acid for 10 min. Images were obtained using a Leica TCS SPE confocal system and a Leica DMi8 fluorescence microscope system using a FITC cube. Multiple images were captured with the 10X objective and stitched to generate images of the brain hemisphere (Leica LAS X software).

Brain sample preparation and immunostaining. Mice were euthanized at 3 or 14 days after stroke. Mice were transcardially perfused with heparinized PBS, followed by 4% PFA (paraformaldehyde in PBS).

Brains were harvested and then fixed for an additional 24 h in 4% PFA at 4 °C. Brains were then transferred to 30% sucrose solution in PBS for 24 h hours prior to generating 30 µm coronal sections (Micron HM 450, Thermo Fisher Scientific, MA, USA). For immunostaining, sections were washed with PBS, incubated with blocking buffer (10% goat serum, 0.3% Trion X-100 in PBS), and then incubated overnight at 4 °C with the following primary antibodies: Rabbit anti-IBA-1 antibody (1:200) (Wako Pure Chemical, Japan), mouse anti-GFAP antibody-cy3 (1:500) (MilliporeSigma, MO, USA). For detection of the IBA-1 antibody, we used either donkey anti-rabbit IgG-Alexa 594 or 488 (1:200, Thermo Fisher Scientific, MA, USA). Sections were incubated with DAPI (4',6-diamidino-2-phenylindole) to label nuclei. Images were obtained using a Leica TCS SPE confocal system and a Leica DMi8 fluorescence microscope system (Leica Biosystem, IL, USA). Multiple images were captured with the 10X objective covering the whole brain or brain hemisphere Sect. (48 images) and stitched to generate a single image (Leica LAS X software). Higher magnification was performed of selected regions using 20X or 40X objectives. Image analysis was performed using ImageJ software (National Institutes of Health).

Identification of CCR2+ cell in brains. pdMCAO was performed on CCR2^{RFP} mice (Jax017586—B6.129(Cg)-CCR2 < tm2.1Ifc > /J, male)³⁵ in which red fluorescent protein is constitutively expressed under the chemokine (C-C motif) receptor 2 (CCR2) promoter. At 2 weeks after surgery, brains were isolated and sectioned as described above. Sections were incubated with DAPI and then imaged and analyzed as described above.

Flow cytometry. Mice (sham and stroke group) were anesthetized with Avertin (2,2,2-Tribromoethanol, Sigma, MO, USA) and transcardially perfused with phosphate-buffered saline (PBS) for 5 min. Brains were isolated and then immediately separated into cortex and thalamus. Brain tissue was then placed in complete Roswell Park Memorial Institute (RPMI) 1640 medium, followed by mechanical and enzymatic digestion with 150 µL collagenase/dispase (1 mg/mL) and 300 µL DNase (10 mg/mL; Roche Diagnostics, IN, USA) for 45 min at 37 °C with mild agitation. The tissue was triturated by pipette, cleared of myelin and cell debris (cell debris removal kit, Miltenyi Biotec, Germany), and then filtered through a 70 µm separation filter. Cells were washed and blocked with mouse Fc Block (eBioscience, CA, USA) prior to staining with primary antibody conjugated fluorophores: CD45-eF450 (# 48-0451-82, eBioscience, CA, USA), CD11b-AF700 (# 101,222, Biolegend, CA, USA). All the antibodies were purchased from Biolegend/eBioscience. For live/dead discrimination, a LIVE/DEAD Fixable Aqua Dead Cell Stain Kit was used according to manufacture instructions (Thermo Fisher Scientific, MA, USA). Cells were briefly fixed in 2% PFA. Data was acquired on a CytoFLEX cytometer (Beckman Coulter, CA, USA) and analyzed using FlowJo (BD Biosciences, OR, USA). No less than 100,000 events were recorded for each sample. Cell type-matched fluorescence minus one (FMO) controls were used to determine the positivity of each antibody.

Data analysis. All the data were expressed as mean ± SEM, except Fig. 3D (median with 95% CI). GraphPad Prism (version 9.1, San Diego, CA) was used to analyze and plot the data. Student's unpaired t-test and paired t-test were used for two group comparisons. A *p*-value < 0.05 was considered statistically significant.

Data availability

All data generated or analyzed during this study are included in this published article.

Received: 4 January 2021; Accepted: 3 June 2021

Published online: 15 June 2021

References

- Moskowitz, M. A., Lo, E. H. & Iadecola, C. The science of stroke: mechanisms in search of treatments. *Neuron* **67**, 181–198. <https://doi.org/10.1016/j.neuron.2010.07.002> (2010).
- Heiss, W. D. The ischemic penumbra: how does tissue injury evolve?. *Ann. N Y Acad. Sci.* **1268**, 26–34. <https://doi.org/10.1111/j.1749-6632.2012.06668.x> (2012).
- Chen, H. *et al.* Oxidative stress in ischemic brain damage: mechanisms of cell death and potential molecular targets for neuroprotection. *Antioxid. Redox. Signal* **14**, 1505–1517. <https://doi.org/10.1089/ars.2010.3576> (2011).
- Dirnagl, U., Iadecola, C. & Moskowitz, M. A. Pathobiology of ischaemic stroke: an integrated view. *Trends Neurosci.* **22**, 391–397 (1999).
- Aggleton, J. P. *et al.* Thalamic pathology and memory loss in early Alzheimer's disease: moving the focus from the medial temporal lobe to Papez circuit. *Brain* **139**, 1877–1890. <https://doi.org/10.1093/brain/aww083> (2016).
- von Cramon, D. Y., Hebel, N. & Schuri, U. A contribution to the anatomical basis of thalamic amnesia. *Brain* **108**(Pt 4), 993–1008. <https://doi.org/10.1093/brain/108.4.993> (1985).
- Kuchcinski, G. *et al.* Thalamic alterations remote to infarct appear as focal iron accumulation and impact clinical outcome. *Brain* **140**, 1932–1946. <https://doi.org/10.1093/brain/awx114> (2017).
- Ogawa, T. *et al.* Secondary thalamic degeneration after cerebral infarction in the middle cerebral artery distribution: evaluation with MR imaging. *Radiology* **204**, 255–262. <https://doi.org/10.1148/radiology.204.1.9205256> (1997).
- Schroeter, M. *et al.* Increased thalamic neurodegeneration following ischaemic cortical stroke in osteopontin-deficient mice. *Brain* **129**, 1426–1437. <https://doi.org/10.1093/brain/awl094> (2006).
- Dihne, M. *et al.* Different mechanisms of secondary neuronal damage in thalamic nuclei after focal cerebral ischemia in rats. *Stroke* **33**, 3006–3011. <https://doi.org/10.1161/01.str.0000039406.64644.cb> (2002).
- Brodtmann, A. *et al.* Dynamic regional brain atrophy rates in the first year after ischemic stroke. *Stroke* **51**, e183–e192. <https://doi.org/10.1161/STROKEAHA.120.030256> (2020).
- Scott, G. *et al.* Thalamic inflammation after brain trauma is associated with thalamo-cortical white matter damage. *J. Neuroinflamm.* **12**, 224. <https://doi.org/10.1186/s12974-015-0445-y> (2015).
- Hunnicut, B. J. *et al.* A comprehensive thalamocortical projection map at the mesoscopic level. *Nat. Neurosci.* **17**, 1276–1285. <https://doi.org/10.1038/nn.3780> (2014).

14. Leyva-Diaz, E. & Lopez-Bendito, G. In and out from the cortex: development of major forebrain connections. *Neuroscience* **254**, 26–44. <https://doi.org/10.1016/j.neuroscience.2013.08.070> (2013).
15. Grant, E., Hoerder-Suabedissen, A. & Molnar, Z. Development of the corticothalamic projections. *Front Neurosci.* **6**, 53. <https://doi.org/10.3389/fnins.2012.00053> (2012).
16. Landisman, C. E. & Connors, B. W. VPM and PoM nuclei of the rat somatosensory thalamus: intrinsic neuronal properties and corticothalamic feedback. *Cereb. Cortex.* **17**, 2853–2865. <https://doi.org/10.1093/cercor/bhm025> (2007).
17. Ohno, S. *et al.* A morphological analysis of thalamocortical axon fibers of rat posterior thalamic nuclei: a single neuron tracing study with viral vectors. *Cereb. Cortex.* **22**, 2840–2857. <https://doi.org/10.1093/cercor/bhr356> (2012).
18. Guillery, R. W. & Sherman, S. M. Thalamic relay functions and their role in corticocortical communication: generalizations from the visual system. *Neuron* **33**, 163–175. [https://doi.org/10.1016/s0896-6273\(01\)00582-7](https://doi.org/10.1016/s0896-6273(01)00582-7) (2002).
19. Fama, R. & Sullivan, E. V. Thalamic structures and associated cognitive functions: Relations with age and aging. *Neurosci. Biobehav. Rev.* **54**, 29–37. <https://doi.org/10.1016/j.neubiorev.2015.03.008> (2015).
20. Redinbaugh, M. J. *et al.* Thalamus modulates consciousness via layer-specific control of cortex. *Neuron* **106**(66–75), e12. <https://doi.org/10.1016/j.neuron.2020.01.005> (2020).
21. Hwang, K. *et al.* The human thalamus is an integrative hub for functional brain networks. *J. Neurosci.* **37**, 5594–5607. <https://doi.org/10.1523/JNEUROSCI.0067-17.2017> (2017).
22. Baumgartner, P. *et al.* Sensorimotor stroke alters hippocampo-thalamic network activity. *Sci. Rep.* **8**, 15770. <https://doi.org/10.1038/s41598-018-34002-9> (2018).
23. Cao, Z. *et al.* TRPV1-mediated pharmacological hypothermia promotes improved functional recovery following ischemic stroke. *Sci. Rep.* **7**, 17685. <https://doi.org/10.1038/s41598-017-17548-y> (2017).
24. Jones, K. A. *et al.* Chronic stress exacerbates neuronal loss associated with secondary neurodegeneration and suppresses microglial-like cells following focal motor cortex ischemia in the mouse. *Brain Behav. Immun.* **48**, 57–67. <https://doi.org/10.1016/j.bbi.2015.02.014> (2015).
25. Ong, L. K. *et al.* Chronic stress exposure following photothrombotic stroke is associated with increased levels of Amyloid beta accumulation and altered oligomerisation at sites of thalamic secondary neurodegeneration in mice. *J. Cereb. Blood Flow Metab.* **37**, 1338–1348. <https://doi.org/10.1177/0271678X16654920> (2017).
26. Otxoa-de-Amezaga, A. *et al.* Microglial cell loss after ischemic stroke favors brain neutrophil accumulation. *Acta Neuropathol.* **137**, 321–341. <https://doi.org/10.1007/s00401-018-1954-4> (2019).
27. Matsumoto, H. *et al.* Antibodies to CD11b, CD68, and lectin label neutrophils rather than microglia in traumatic and ischemic brain lesions. *J. Neurosci. Res.* **85**, 994–1009. <https://doi.org/10.1002/jnr.21198> (2007).
28. Yu, L. *et al.* Microglia and Their promising role in ischemic brain injuries: an update. *Front Cell Neurosci.* **14**, 211. <https://doi.org/10.3389/fncel.2020.00211> (2020).
29. Taylor, R. A. & Sansing, L. H. Microglial responses after ischemic stroke and intracerebral hemorrhage. *Clin. Dev. Immunol.* **2013**, 746068. <https://doi.org/10.1155/2013/746068> (2013).
30. Zuo, X. *et al.* Inhibition of cathepsin B alleviates secondary degeneration in ipsilateral thalamus after focal cerebral infarction in adult rats. *J. Neuropathol. Exp. Neurol.* **75**, 816–826. <https://doi.org/10.1093/jnen/nlw054> (2016).
31. Weishaupt, N. *et al.* Prefrontal ischemia in the rat leads to secondary damage and inflammation in remote gray and white matter regions. *Front Neurosci.* **10**, 81. <https://doi.org/10.3389/fnins.2016.00081> (2016).
32. Ling, L. *et al.* Neurogenesis and angiogenesis within the ipsilateral thalamus with secondary damage after focal cortical infarction in hypertensive rats. *J. Cereb. Blood Flow Metab.* **29**, 1538–1546. <https://doi.org/10.1038/jcbfm.2009.76> (2009).
33. Gelderblom, M. *et al.* Temporal and spatial dynamics of cerebral immune cell accumulation in stroke. *Stroke* **40**, 1849–1857. <https://doi.org/10.1161/STROKEAHA.108.534503> (2009).
34. Miro-Mur, F. *et al.* Immature monocytes recruited to the ischemic mouse brain differentiate into macrophages with features of alternative activation. *Brain Behav. Immun.* **53**, 18–33. <https://doi.org/10.1016/j.bbi.2015.08.010> (2016).
35. Saederup, N. *et al.* Selective chemokine receptor usage by central nervous system myeloid cells in CCR2-red fluorescent protein knock-in mice. *PLoS ONE* **5**, e13693. <https://doi.org/10.1371/journal.pone.0013693> (2010).
36. Sims, N. R. & Yew, W. P. Reactive astrogliosis in stroke: contributions of astrocytes to recovery of neurological function. *Neurochem. Int.* **107**, 88–103. <https://doi.org/10.1016/j.neuint.2016.12.016> (2017).
37. Hammond, T. R. *et al.* Single-cell RNA sequencing of microglia throughout the mouse lifespan and in the injured brain reveals complex cell-state changes. *Immunity* **50**(253–271), e256. <https://doi.org/10.1016/j.immuni.2018.11.004> (2019).
38. Grabert, K. *et al.* Microglial brain region-dependent diversity and selective regional sensitivities to aging. *Nat. Neurosci.* **19**, 504–516. <https://doi.org/10.1038/nn.4222> (2016).
39. Koellhoffer, E. C., McCullough, L. D. & Ritzel, R. M. Old maids: aging and its impact on microglia function. *Int. J. Mol. Sci.* <https://doi.org/10.3390/ijms18040769> (2017).
40. Moraga, A. *et al.* Aging increases microglial proliferation, delays cell migration, and decreases cortical neurogenesis after focal cerebral ischemia. *J. Neuroinflamm.* **12**, 87. <https://doi.org/10.1186/s12974-015-0314-8> (2015).
41. Pietrogrande, G. *et al.* Low oxygen post conditioning prevents thalamic secondary neuronal loss caused by excitotoxicity after cortical stroke. *Sci. Rep.* **9**, 4841. <https://doi.org/10.1038/s41598-019-39493-8> (2019).
42. Chen, B. *et al.* Memantine attenuates cell apoptosis by suppressing the calpain-caspase-3 pathway in an experimental model of ischemic stroke. *Exp. Cell Res.* **351**, 163–172. <https://doi.org/10.1016/j.yexcr.2016.12.028> (2017).
43. Trotman, M. *et al.* The dichotomy of memantine treatment for ischemic stroke: dose-dependent protective and detrimental effects. *J. Cereb. Blood Flow Metab.* **35**, 230–239. <https://doi.org/10.1038/jcbfm.2014.188> (2015).
44. Gorgulu, A. *et al.* Reduction of edema and infarction by Memantine and MK-801 after focal cerebral ischaemia and reperfusion in rat. *Acta Neurochir. (Wien)* **142**, 1287–1292. <https://doi.org/10.1007/s007010070027> (2000).
45. Weinstein, J. R., Koerner, I. P. & Moller, T. Microglia in ischemic brain injury. *Future Neurol.* **5**, 227–246. <https://doi.org/10.2217/fnl.10.1> (2010).
46. Benakis, C. *et al.* The role of microglia and myeloid immune cells in acute cerebral ischemia. *Front Cell Neurosci.* **8**, 461. <https://doi.org/10.3389/fncel.2014.00461> (2014).
47. Hu, X. *et al.* Microglia/macrophage polarization dynamics reveal novel mechanism of injury expansion after focal cerebral ischemia. *Stroke* **43**, 3063–3070. <https://doi.org/10.1161/STROKEAHA.112.659656> (2012).
48. Hu, X. *et al.* Microglial and macrophage polarization-new prospects for brain repair. *Nat. Rev. Neurol.* **11**, 56–64. <https://doi.org/10.1038/nrneurol.2014.207> (2015).
49. Sapkota, A. *et al.* Eupatilin exerts neuroprotective effects in mice with transient focal cerebral ischemia by reducing microglial activation. *PLoS ONE* **12**, e0171479. <https://doi.org/10.1371/journal.pone.0171479> (2017).
50. Moraga, A. *et al.* Imaging the role of toll-like receptor 4 on cell proliferation and inflammation after cerebral ischemia by positron emission tomography. *J. Cereb. Blood Flow Metab.* **36**, 702–708. <https://doi.org/10.1177/0271678X15627657> (2016).
51. Khan, A. *et al.* Transcriptomic analysis reveals differential activation of microglial genes after ischemic stroke in mice. *Neuroscience* **348**, 212–227. <https://doi.org/10.1016/j.neuroscience.2017.02.019> (2017).
52. Hess, D. C. *et al.* Hematopoietic origin of microglial and perivascular cells in brain. *Exp. Neurol.* **186**, 134–144. <https://doi.org/10.1016/j.expneurol.2003.11.005> (2004).

53. Chen, H. R. *et al.* Fate mapping via CCR2-CreER mice reveals monocyte-to-microglia transition in development and neonatal stroke. *Sci. Adv.* **6**, eabb2119. <https://doi.org/10.1126/sciadv.abb2119> (2020).
54. Watanabe, S. *et al.* The role of macrophages in the resolution of inflammation. *J. Clin. Invest.* **129**, 2619–2628. <https://doi.org/10.1172/JCI124615> (2019).
55. Ladwig, A. *et al.* Osteopontin attenuates secondary neurodegeneration in the thalamus after experimental stroke. *J. Neuroimmune Pharmacol.* **14**, 295–311. <https://doi.org/10.1007/s11481-018-9826-1> (2019).
56. Roger, V. L. *et al.* Executive summary: heart disease and stroke statistics–2012 update: a report from the American Heart Association. *Circulation* **125**, 188–197. <https://doi.org/10.1161/CIR.0b013e3182456d46> (2012).
57. Mitchell, S. J. *et al.* Animal models of aging research: implications for human aging and age-related diseases. *Annu. Rev. Anim. Biosci.* **3**, 283–303. <https://doi.org/10.1146/annurev-animal-022114-110829> (2015).
58. Dutta, S. & Sengupta, P. Men and mice: relating their ages. *Life Sci.* **152**, 244–248. <https://doi.org/10.1016/j.lfs.2015.10.025> (2016).
59. Sohrabji, F., Bake, S. & Lewis, D. K. Age-related changes in brain support cells: Implications for stroke severity. *Neurochem. Int.* **63**, 291–301. <https://doi.org/10.1016/j.neuint.2013.06.013> (2013).
60. Niraula, A., Sheridan, J. F. & Godbout, J. P. Microglia Priming with aging and stress. *Neuropsychopharmacology* **42**, 318–333. <https://doi.org/10.1038/npp.2016.185> (2017).
61. Henry, C. J. *et al.* Peripheral lipopolysaccharide (LPS) challenge promotes microglial hyperactivity in aged mice that is associated with exaggerated induction of both pro-inflammatory IL-1beta and anti-inflammatory IL-10 cytokines. *Brain Behav. Immun.* **23**, 309–317. <https://doi.org/10.1016/j.bbi.2008.09.002> (2009).
62. Streit, W. J. *et al.* Dystrophic microglia in the aging human brain. *Glia* **45**, 208–212. <https://doi.org/10.1002/glia.10319> (2004).
63. Miller, K. R. & Streit, W. J. The effects of aging, injury and disease on microglial function: a case for cellular senescence. *Neuron. Glia Biol.* **3**, 245–253. <https://doi.org/10.1017/S1740925X08000136> (2007).
64. Flanary, B. E. & Streit, W. J. Telomeres shorten with age in rat cerebellum and cortex in vivo. *J. Anti. Aging Med.* **6**, 299–308. <https://doi.org/10.1089/109454503323028894> (2003).
65. Silver, J. & Miller, J. H. Regeneration beyond the glial scar. *Nat. Rev. Neurosci.* **5**, 146–156. <https://doi.org/10.1038/nrn1326> (2004).
66. Wanner, I. B. *et al.* Glial scar borders are formed by newly proliferated, elongated astrocytes that interact to corral inflammatory and fibrotic cells via STAT3-dependent mechanisms after spinal cord injury. *J. Neurosci.* **33**, 12870–12886. <https://doi.org/10.1523/JNEUROSCI.12121-13.2013> (2013).
67. Adams, K. L. & Gallo, V. The diversity and disparity of the glial scar. *Nat. Neurosci.* **21**, 9–15. <https://doi.org/10.1038/s41593-017-0033-9> (2018).
68. Cai, H. *et al.* Hypoxia response element-regulated MMP-9 promotes neurological recovery via glial scar degradation and angiogenesis in delayed stroke. *Mol. Ther.* **25**, 1448–1459. <https://doi.org/10.1016/j.yjth.2017.03.020> (2017).
69. Anderson, M. A. *et al.* Astrocyte scar formation aids central nervous system axon regeneration. *Nature* **532**, 195–200. <https://doi.org/10.1038/nature17623> (2016).
70. Huang, L. *et al.* Glial scar formation occurs in the human brain after ischemic stroke. *Int. J. Med. Sci.* **11**, 344–348. <https://doi.org/10.7150/ijms.8140> (2014).
71. Liddelow, S. A. & Barres, B. A. Reactive astrocytes: production, function, and therapeutic potential. *Immunity* **46**, 957–967. <https://doi.org/10.1016/j.immuni.2017.06.006> (2017).
72. Sofroniew, M. V. Astrocyte barriers to neurotoxic inflammation. *Nat. Rev. Neurosci.* **16**, 249–263. <https://doi.org/10.1038/nrn3898> (2015).
73. Herrmann, J. E. *et al.* STAT3 is a critical regulator of astrogliosis and scar formation after spinal cord injury. *J. Neurosci.* **28**, 7231–7243. <https://doi.org/10.1523/JNEUROSCI.1709-08.2008> (2008).
74. Erik, J. *et al.* Cross-talk between monocyte invasion and astrocyte proliferation regulates scarring in brain injury. *EMBO Rep.* <https://doi.org/10.15252/embr.201745294> (2018).
75. Zeisel, A. *et al.* Molecular architecture of the mouse nervous system. *Cell* **174**(999–1014), e1022. <https://doi.org/10.1016/j.cell.2018.06.021> (2018).
76. Avey, D. *et al.* Single-cell RNA-seq uncovers a robust transcriptional response to morphine by glia. *Cell Rep.* **24**(3619–3629), e3614. <https://doi.org/10.1016/j.celrep.2018.08.080> (2018).
77. Becerra-Calixto, A. & Cardona-Gomez, G. P. The role of astrocytes in neuroprotection after brain stroke: potential in cell therapy. *Front Mol. Neurosci.* **10**, 88. <https://doi.org/10.3389/fnmol.2017.00088> (2017).
78. Wang, H. *et al.* Portrait of glial scar in neurological diseases. *Int. J. Immunopathol. Pharmacol.* **31**, 2058738418801406. <https://doi.org/10.1177/2058738418801406> (2018).
79. Gupta, N. & Pandey, S. Post-thalamic stroke movement disorders: a systematic review. *Eur. Neurol.* **79**, 303–314. <https://doi.org/10.1159/000490070> (2018).
80. Molinuevo, J. L., Llado, A. & Rami, L. Memantine: targeting glutamate excitotoxicity in Alzheimer's disease and other dementias. *Am. J. Alzheimers Dis. Other Demen.* **20**, 77–85. <https://doi.org/10.1177/153331750502000206> (2005).
81. Ross, D. T. & Ebner, F. F. Thalamic retrograde degeneration following cortical injury: An excitotoxic process?. *Neuroscience* **35**, 525–550. [https://doi.org/10.1016/0306-4522\(90\)90327-z](https://doi.org/10.1016/0306-4522(90)90327-z) (1990).
82. Liu, M. *et al.* Role of P450 aromatase in sex-specific astrocytic cell death. *J. Cereb. Blood Flow Metab.* **27**, 135–141. <https://doi.org/10.1038/sj.cbfm.9600331> (2007).
83. Chisholm, N. C. & Sohrabji, F. Astrocytic response to cerebral ischemia is influenced by sex differences and impaired by aging. *Neurobiol. Dis.* **85**, 245–253. <https://doi.org/10.1016/j.nbd.2015.03.028> (2016).
84. Manwani, B. *et al.* Differential effects of aging and sex on stroke induced inflammation across the lifespan. *Exp. Neurol.* **249**, 120–131. <https://doi.org/10.1016/j.expneurol.2013.08.011> (2013).

Acknowledgements

This project was funded by NIH NS096186 (S.P.M) and NS 094280 (S.P.M).

Author contributions

S.P.M. and G.S.K. conceived the experiments. G.S.K., J.M.S., A.A.M., T.W. performed the experiments. G.S.K., S.P.M., J.L. and F.L. analyzed the results. S.P.M., G.S.K., M.G.G. and J.W.M. discussed the results. S.P.M. and G.S.K. made the figures and wrote the manuscript. All authors reviewed the manuscript.

Competing interests

The authors declare no competing interests.

Additional information

Supplementary Information The online version contains supplementary material available at <https://doi.org/10.1038/s41598-021-91998-3>.

Correspondence and requests for materials should be addressed to S.P.M.

Reprints and permissions information is available at www.nature.com/reprints.

Publisher's note Springer Nature remains neutral with regard to jurisdictional claims in published maps and institutional affiliations.



Open Access This article is licensed under a Creative Commons Attribution 4.0 International License, which permits use, sharing, adaptation, distribution and reproduction in any medium or format, as long as you give appropriate credit to the original author(s) and the source, provide a link to the Creative Commons licence, and indicate if changes were made. The images or other third party material in this article are included in the article's Creative Commons licence, unless indicated otherwise in a credit line to the material. If material is not included in the article's Creative Commons licence and your intended use is not permitted by statutory regulation or exceeds the permitted use, you will need to obtain permission directly from the copyright holder. To view a copy of this licence, visit <http://creativecommons.org/licenses/by/4.0/>.

© The Author(s) 2021